

Spectroscopic study of Ga–In–P based self-organized lateral superlattices

Sandip Ghosh[†]§, B M Arora[†], Seong-Jin Kim[‡], Joo-Hyong Noh[‡]
and Hajime Asahi[‡]

[†] Solid State Electronics Group, Tata Institute of Fundamental Research,
Homi Bhabha Road, Colaba, Mumbai 400 005, India

[‡] The Institute of Scientific and Industrial Research, Osaka University, 8-1 Mihogaoka,
Ibaraki, Osaka 567, Japan

Received 16 July 1998, accepted for publication 11 December 1998

Abstract. This paper reports polarization and temperature dependent contactless electroreflectance (CER) and photoluminescence (PL) study of strain compensated short period (GaP)₂(InP)₂ superlattices on GaAs(001) substrates which show self-organized lateral composition modulation (LCM) in the form of alternate In/Ga rich regions along the [110] direction in the (001) plane. The LCM related PL peak position is at a lower energy as compared to the corresponding feature in the CER spectrum and the difference is found to be the same as the activation energy for thermal quenching of the PL signal. These results have been explained by suggesting that the PL signal arises mainly from recombination of carriers localized at potential fluctuations (In rich regions with excessively high In concentration) within the lateral superlattice (LS) structure that is formed due to the LCM while the CER feature arises from transitions between the minibands of the average LS structure. The PL signal is quenched due to thermal excitation of the carriers from these excessively In rich regions into the minibands. The LS band gap energy is accurately determined and its implication for the random alloy model used to describe the electronic band structure of such systems is discussed. The temperature dependences of critical point energies have also been measured and analysed.

1. Introduction

Self-organized semiconductor quantum wires and superlattices have received considerable attention due to their novel physical properties and scope for device applications [1]. In this context (GaP)_n(InP)_m strain compensated short period vertical superlattices (VSs) grown on GaAs(001) substrates are of interest since in these samples, depending on the individual InP and GaP monolayer numbers (*n*, *m*), there occurs lateral composition modulation (LCM) resulting in the formation of alternate lamellae of Ga rich and In rich regions parallel to the [110] direction in the (001) plane. Evidence for LCM has been obtained from transmission electron microscopy (TEM) and energy dispersive x-ray analysis (EDX) measurements [2]. It has been proposed that the process leading to the lateral composition modulation is initiated by strongly anisotropic diffusion of the group III atoms on GaAs(001) surface and thereafter sustained by strain induced nucleation of excess adatoms [3]. However the detailed nature of this strain induced lateral ordering mechanism still remains unresolved as it cannot explain why the wavelength of the LCM (typically $\simeq 100$ to 400 Å) and its amplitude

(typically $\simeq 10\%$ to 20% excess concentration over average) are nearly the same in most material systems where such a phenomenon is observed [1].

The most dramatic effect of LCM is seen in the electronic band structure of these samples. A large shift of the photoluminescence (PL) peak position to lower energy has been observed in these samples and has been explained by suggesting that LCM leads to the formation of a lateral superlattice (LS) and the PL signal arises from carrier recombination in the In rich low energy well regions of the LS. Strongly polarization sensitive optical properties have also been reported and put forth as evidence for LCM [4–6]. A theoretical model which considers the Ga and the In rich regions as coherently strained random Ga_xIn_{1-x}P alloys has been used to describe the electronic band structure of these materials. However the transition energies obtained on the basis of this random alloy model do not match the experimental values based on PL measurements [5]. In this paper through a combination of polarization and temperature dependent contactless electroreflectance (CER) and PL measurements we probe the origins and the decay pathway of the luminescence signals from these samples and discuss them in relation to the proposed random alloy model. Thereafter we present and analyse some interesting data on

§ Present address: Physics Department, University of Surrey, Guildford GU2 5XH, UK.

the temperature dependence of the transition energy of the LCM related feature in the CER spectrum of these samples.

2. Experiment

Using gas source molecular beam epitaxy we have grown several samples with different GaP/InP monolayer numbers and on differently oriented GaAs substrates [7, 8]. From amongst them the present study concentrates on the sample where LCM shows up most prominently and for which theoretical calculations based on the random alloy model exist in the literature. The sample structure is shown schematically in figure 1(a). It consists of a $\simeq 0.3 \mu\text{m}$ thick $(\text{GaP})_2(\text{InP})_2$ short period vertical superlattice (VS) grown on an n^+ GaAs(001) substrate with a non-intentionally doped GaAs buffer in between. The TEM picture of the sample surface in figure 1(b) shows alternating wire-like bright and dark patches oriented along the $[\bar{1}10]$ direction. The cross-sectional TEM pictures (not shown here) of the $(\bar{1}10)$ plane indicate that these patches extend vertically in the $[001]$ direction. A higher resolution scanning tunnelling microscope (STM) picture of the surface shown in figure 1(c) reveals that these patches have an average thickness of $\simeq 60 \text{ \AA}$. Detailed STM studies on these samples reported earlier [8] showed that the dark regions were Ga rich while the bright regions were In rich. EDX measurements performed on similar samples [5] have shown that the In rich regions have an average In concentration of $\simeq 60\%$, while in the In deficient regions the average In concentration is $\simeq 40\%$. These structural characteristics of our sample are identical to those reported by Pearah *et al* [5].

In the PL experiments the excitation source was either a 2 mW He-Ne laser (632.8 nm) or a 20 mW Ar^+ ion laser (488 nm). The luminescence was detected using a photomultiplier tube after it was dispersed by a $1/8 \text{ m}$ monochromator with 1 nm band pass. The sample was cooled using a closed cycle helium refrigerator. In the CER [9] measurements, the sample was placed between two electrodes in a capacitor-like arrangement with the top electrode kept $\simeq 0.3 \text{ mm}$ from the sample surface. A 1 kV (r.m.s.) sinusoidal voltage was applied on the top transparent electrode to modulate the sample's surface electric field. The probe beam was obtained by dispersing light from a 150 W QTH lamp using a $1/8 \text{ m}$ monochromator with $\simeq 4 \text{ nm}$ bandpass and detected using a silicon photodetector. In all cases a broad band polymer film polarizer was used to polarize the incident light and to analyse the polarization characteristics of the output light. In each case the polarization dependence of the monochromator's grating response was separately measured and corrected for.

3. Results and discussion

3.1. Origins of CER and PL signals

Figure 2(a) shows the PL spectrum of the sample at 9 K with an unpolarized He-Ne laser as the excitation source. The dashed line represents the component of the PL spectrum with the electric vector parallel to the $[\bar{1}10]$ direction and the dotted line that along $[110]$. The peak around 1.51 eV

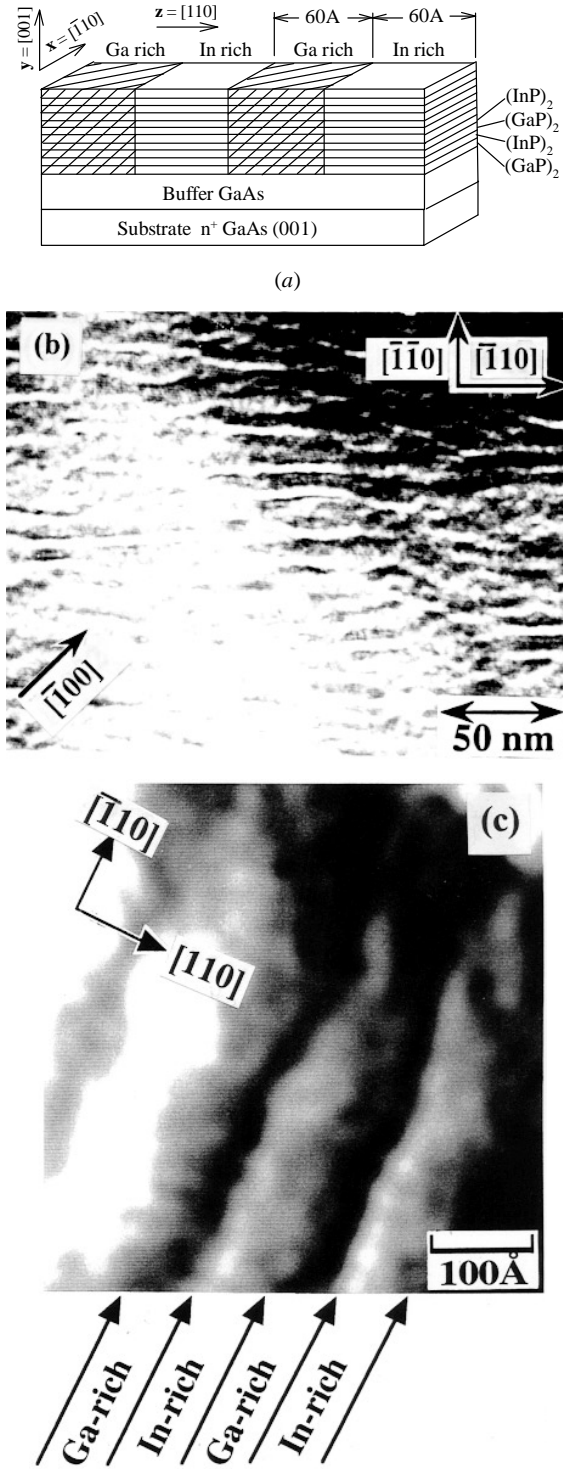


Figure 1. (a) Schematic of the sample structure. (b) TEM picture of the sample surface. (c) Higher resolution STM picture of the sample surface.

is due to the GaAs buffer and substrate. This feature has negligible polarization dependence since for a crystal with zinc blende symmetry the two directions $[\bar{1}10]$ and $[110]$ are identical. In contrast the next peak around 1.68 eV shows a strong polarization dependence; the peak height being reduced by a factor of $\simeq 7$ for the component along

[110] as compared to the component along $[\bar{1}10]$. Figure 2(b) shows the CER spectrum of the sample at 9 K. In plot (i) the polarization of the incident probe beam is parallel to the $[\bar{1}10]$ direction. The features in this spectrum between 1.5 and 1.6 eV are Franz–Keldysh oscillations (FKO) arising from the buffer/substrate GaAs layers. We shall refer to the feature between 1.65 and 1.8 eV as A1 and that between 1.85 and 1.9 eV as B. In plot (ii) the polarization of the incident probe beam is parallel to [110]. In this spectrum the GaAs FKO and the feature B show negligible change. However, the feature A1, seen earlier with the $[\bar{1}10]$ polarized light between 1.65 and 1.8 eV, is no longer present and in its place there is a weak and much broader feature which we shall refer to as A2. To estimate the transition energies we fitted to these spectral features the lineshape function given by

$$\Delta R/R = \sum_{j=1}^n \text{Re} [a_j \exp(i\theta_j)/(E - E_{0j} + i\Gamma_j)^m] \quad (1)$$

$$i = \sqrt{-1}$$

where E_{0j} , Γ_j , θ_j and a_j are the transition energy, broadening parameter, phase factor and amplitude respectively, associated with the j th transition. The above equation with $m = 3$, which mimics the case of a first derivative Gaussian broadened lineshape function [10], fits our data best indicating inhomogeneous broadening of the critical point energies in these samples. The fitted curves are shown by the dash–double dot lines in figure 2(b). The values of E_0 and Γ for A1 were found to be 1.728 eV and 47 meV while those for feature B were found to be 1.877 eV and 21 meV respectively. Although the presence of the feature A2 for light polarized along [110] is unambiguous, its weak strength as compared to the background causes the parameter values obtained by lineshape fitting to be unreliable.

By comparison with the work of Armelles *et al* [11] on $(\text{GaP})_n(\text{InP})_m$ superlattices, the polarization independent CER feature B and the associated weak PL feature at ≈ 1.86 eV (in the inset of figure 2(a)) are easily identified as the signatures of the $(\text{GaP})_2(\text{InP})_2$ VS. The polarized PL signal has previously been identified as arising due to carrier recombination in the In rich low energy well regions of the LS formed as result of the composition modulation [5]. The presence of signatures of both the VS and the LS suggests that the composition modulation is not uniform throughout the sample i.e. the self-organization process gives rise to two distinct phases in the sample, one where the lateral composition modulation predominates (LS) and one where the original structure is relatively undisturbed (VS). Pearah *et al* [5] explained the polarization dependence of the PL originating in the LS on the basis of strains in the Ga/In rich regions. Recently Ghosh *et al* [6] have suggested another possible explanation for the polarization anisotropy of the CER feature A1 that is associated with the LCM in the sample which briefly is as follows. At the valence band edge of the III–V semiconductors with zinc blende structure, the cell periodic parts of the heavy hole (hh) and the light hole (lh) wavefunctions can be described using the p_x , p_y and p_z atomic orbitals. The hh wavefunction does not have a p_z component so that light polarized parallel to \hat{z} cannot excite an hh transition although it can excite an lh transition. Under normal conditions the hh and the lh

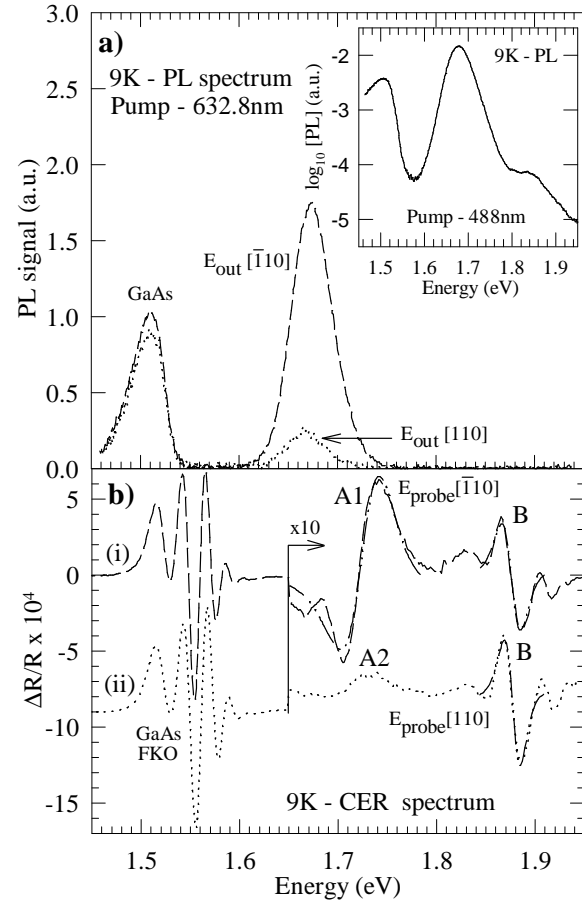


Figure 2. (a) Photoluminescence (PL) output signal from the sample polarized along $[\bar{1}10]$ (dashed line) and along [110] (dotted line). The excitation source (pump) was an unpolarized He–Ne laser (632.8 nm). The inset shows a logarithmic plot of the PL signal (consisting of both the [110] and $[\bar{1}10]$ polarized components) obtained with a Ar^+ ion laser (488 nm) pump beam polarized at 45° to $[\bar{1}10]$. (b) Contactless electroreflectance spectrum of the sample for $[\bar{1}10]$ and [110] polarizations of the incident probe beam. The plots are vertically shifted for clarity. The dash–double dot lines represent fits to equation (1).

states are degenerate at the valence band edge and there is no preferred \hat{z} direction, therefore no optical anisotropy is observed. However quantum confinement in superlattices and quantum wells splits the hh and the lh states while the confinement direction defines the \hat{z} direction [12]. So if light is incident in a way such that it can be polarized both in the plane of the well and perpendicular to it, then the relative intensities of various lines in the spectrum can change depending on the polarization [13]. In the present case quantum confinement in the LS lifts the degeneracy between the lh and the hh states and the LS potential also defines the preferred \hat{z} direction as [110]. Therefore an hh transition in the LS would not be excited for light polarization along [110], the direction perpendicular to the LS planes, while it would be excited for light polarized along $[\bar{1}10]$, which lies in the LS planes. This is exactly how the feature A1 behaves and therefore was identified as arising from the lowest hh transition in the LS. The weak feature A2 was identified as being associated with a lh transition as it is

present even when the incident polarization is along [110] i.e. the \hat{z} direction. The transition matrix elements which determine the polarization selection rules being the same for both the emission and the absorption processes, the PL output originating mainly from hh recombinations is expected to be strongly polarized along $[\bar{1}10]$ which is what we observe. A signature of the LS barrier is not seen in the CER spectrum most likely because in a superlattice, the barrier band gap does not correspond to a particularly large change in the joint density of states [12]. Also the identification of the feature B in CER as being the signature of the $(\text{GaP})_2(\text{InP})_2$ VS phase explains its relative polarization insensitivity because for this structure both the [110] and $[\bar{1}10]$ polarizations lie in the plane of the VS.

From the point of view of the present study it is important to note that the LCM related PL peak position (1.68 eV) is lower than the corresponding CER transition energy (feature A1 at 1.728 eV) by 48 meV. In order to further study the PL process, we have investigated the temperature dependence of the total integrated PL output. From figure 2(a) and the related discussion above, the total PL output at 1.68 eV can be considered to be arising mainly from hh recombinations. The open circles in figure 3(a) show a logarithmic plot of the integrated PL output of our sample as a function of inverse of temperature in the range 9 to 90 K. The continuous line represents a fit to the data using the following equation [14]:

$$I(T)_{PL} = I_0/[1 + \gamma \exp(-Q/k_B T)] \quad (2)$$

where $I(T)_{PL}$ is the integrated PL intensity at a given temperature T , Q the activation energy for PL quenching, I_0 the intensity at the lowest temperature and γ has been interpreted as the ratio of the radiative lifetime to the minimum non-radiative life time for carrier decay. The values of γ and Q were found to be $4_{-2}^{+4} \times 10^4$ and 45 ± 4 meV respectively. This activation energy for thermal quenching of PL is identical to (within error bars) the 48 meV energy difference observed between the PL peak position and the CER transition energy associated with the LS. We suggest that this is not a coincidence and that it can be explained as follows.

Before detailing our argument we note the following. In the case of quantum wells (QW) it is found that the activation energy for PL quenching, as obtained from the temperature dependence of the integrated PL intensity, is equal to the difference between the PL emission energy and the barrier band gap [15], indicating that the PL quenching mechanism involves simultaneous thermal emission of the electron and the hole constituting the exciton into energy levels corresponding to the adjacent barriers from where they can recombine either radiatively or non-radiatively, the latter process being dominant more often. The barrier energy essentially represents a state to which carriers may be thermally emitted and lost. Also recently it has been shown that the origin of luminescence and lasing from $\text{Ga}_x\text{In}_{1-x}\text{N}$ based structures, in spite of the high defect densities in them, is due to the recombination of carriers localized in In rich (low energy) regions within these structures [16]. As a consequence of their localization in a small region (as opposed to their being in extended states) the carriers

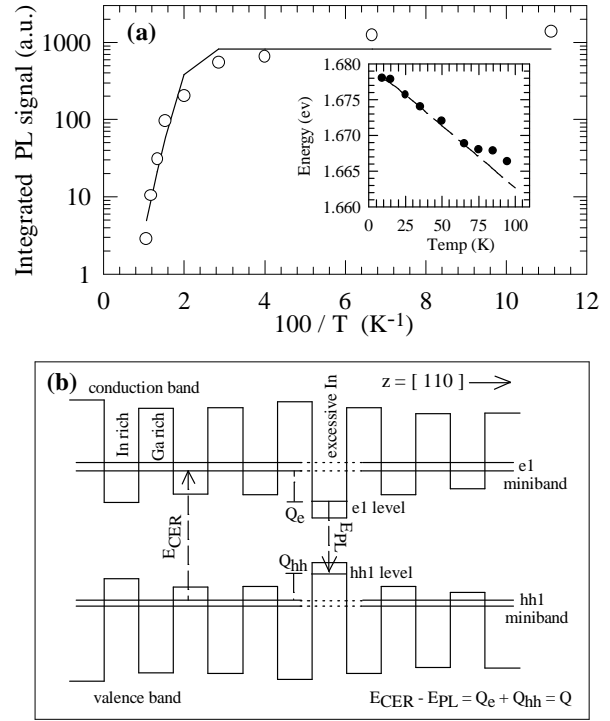


Figure 3. (a) The temperature dependence of the integrated photoluminescence intensity. The circles are experimental points and the line is a fit to equation (2). The inset shows the temperature dependence of the PL peak position (circles) which deviates from the expected regular decrease with increase in temperature (dashed line) beyond 75 K. (b) Schematic showing the origins of the CER and PL transitions. Seen in the figure are potential fluctuations caused by variations in the In content of the well region as well as the minibands of the lateral superlattice.

do not encounter the defects in the rest of the crystal and so the probability of non-radiative recombination is reduced considerably.

Taking a clue from the above findings we suggest that in the present case the luminescence at low temperature arises due to the recombination of electron–hh pairs localized in some excessively In rich regions (defects) within the LS phase. These regions have more In than the average In concentration in the In rich wells of the LS and consequently lower energy as shown in figure 3(b). On the other hand the CER transition energy A1 corresponds to the hh band gap of the average LS structure which is just the difference between the lowest electron and the highest hh miniband edges of the LS. The In excess low energy regions have high occupation probability at low temperatures so the PL signal arises mainly from carriers recombining in these regions. On the other hand the minibands which lie at a higher energy have lower occupation probabilities at low temperatures. Furthermore they being extended states, the carriers in these states encounter more defects so the non-radiative recombination rates are expected to be higher. Therefore at low temperatures we see no PL peak at the energy corresponding to the difference between the miniband edges. However as the temperature is raised, the carriers localized in the low energy regions are thermally excited

Table 1. The fitted values of the parameters in equation (3) and (4) describing the temperature dependence of the transition energies of features A1 and B in the CER spectrum. The errors in the parameter values are from the fitting procedure. The fitted parameter values for a random $\text{Ga}_x\text{In}_{1-x}\text{P}$ alloy are also given for comparison.

Structure	E_{g0}^V (eV)	$\alpha \times 10^4$ (eV K ⁻¹)	β (K)	E_{g0}^{BE} (eV)	a_{c-phn} (meV)	E_{phn} (meV)
$\text{In}_{0.49}\text{Ga}_{0.51}\text{P}$ alloy	2.009 ± 0.001	8.4 ± 1	515 ± 51	2.007 ± 0.001	64 ± 2	23 ± 1
Vertical superlattice	1.881 ± 0.001	9 ± 2	480 ± 165	1.878 ± 0.001	67 ± 7	22 ± 2
Lateral superlattice	1.733 ± 0.003	4.4 ± 0.3	41 ± 19	1.731 ± 0.002	17 ± 5	7 ± 2

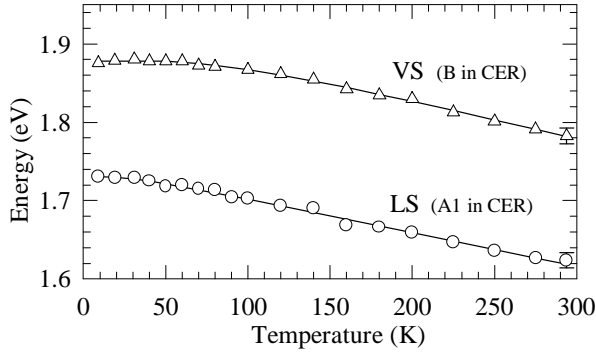


Figure 4. Temperature dependence of the VS (feature B in the CER spectra shown in figure 2(b)) transition energy (triangles) and the LS heavy hole (feature A1 in figure 2(b)) transition energy (circles). The continuous lines are fits to the data using the Bose–Einstein statistics based relation given in equation (4).

into the minibands resulting in the quenching of the PL signal. Once in the minibands the carriers can recombine both radiatively as well as non-radiatively. In the former case it can lead to a shift of the PL peak to higher energies as the temperature is raised. This phenomenon is indeed observed in the present case. The inset in figure 3(a) shows the temperature dependence of the PL peak position. It is evident that beyond 75 K the PL peak energy position shows a clear deviation from its expected regular decrease (dashed line) with increase in temperature. No PL signal could be detected beyond 90 K. In CER, where upward transitions are involved, the dominant factor determining the presence of a spectral feature is the joint density of states (JDOS) rather than the occupation probability. Since the JDOS corresponding to the average LS structure is expected to be much larger than that for the fewer low energy regions due to excessive In concentration, in CER we see a signature of the former and the not the latter. The above assignments explain why the difference between the PL peak energy and the CER transition energy at low temperatures is equal to the activation energy for thermal quenching of PL. We note that the potential fluctuations within the LS such as an increase in the potential well depth (excessively high In concentration) and also width (broader In rich regions) as shown in figure 3(b) still preserve the anisotropy introduced by the LS which explains why the PL continues to be polarized.

In order to theoretically estimate the optical transition energies in the lateral superlattice Pearah *et al* [5] originally used a model which considered the In rich and the Ga rich regions to be disordered $\text{Ga}_x\text{In}_{1-x}\text{P}$ alloys coherently strained with respect to the GaAs substrate. However they found that by using an In composition contrast of $\simeq 60\%/40\%$

between the In rich and the In deficient (Ga rich) regions, they could not match the lowest calculated transition energy with the PL peak at $\simeq 1.68$ eV. More recent calculations of Tang *et al* [17] using a similar model estimate the strained In rich well region of the LS to have a band gap of 1.802 eV at room temperature and the optical transition energy in the LS, when the effects of confinement and lowering of temperature are included, will reach $\simeq 1.83$ eV at 87 K. It is clear that the above model calculations cannot reproduce the 1.68 eV PL emission observed by us and Pearah *et al*. To explain this discrepancy, Pearah *et al* originally made the suggestion that the PL spectrum was dominated by emission from low energy regions resulting from inhomogeneities in the composition modulation. Our above observations prove that this is indeed true, i.e. the actual band gap is higher than the PL peak position. However this difference as we have shown above is just $\simeq 46$ meV, which still leaves an unaccounted difference of $\simeq 100$ meV between the experiment and the model calculation.

Thus our results suggest the need for an improved theoretical model to describe the band structure of this material. In this context the possibilities are (i) a much higher In composition contrast ($\simeq 79\%/21\%$) [5] between the well and the barrier regions, which however seems unlikely considering the results of EDX measurements; (ii) discard the assumption that the In rich and the Ga rich regions are disordered $\text{Ga}_x\text{In}_{1-x}\text{P}$ alloys and instead consider the vertical superlattice structure remaining essentially intact albeit with redistribution of Ga and In in the group III planes forming a lateral superstructure of alternate Ga rich ($(\text{GaP})_{2+\delta}(\text{InP})_{2-\delta}$) and In rich ($(\text{GaP})_{2-\delta}(\text{InP})_{2+\delta}$) regions. The latter would be structurally closer to reality as observed in the high resolution cross-sectional TEM pictures which show that the original vertical superlattice structure essentially remains intact with the InP layers being thicker in one region and the GaP layers being thicker in the adjacent regions [1, 2]. Moreover, the vertical order can provide for the lowering of the energy scale required to match the results of PL and CER measurements since at low temperatures, the band gap of the $(\text{GaP})_2(\text{InP})_2$ vertical superlattice (feature B in figure 2(b)) as measured by us is lower than that of the disordered $\text{In}_{0.49}\text{Ga}_{0.51}\text{P}$ alloy ($E_g = 2$ eV) by $\simeq 125$ meV.

3.2. Temperature dependence of transition energies

Finally we present some interesting results on the temperature dependence of the critical point transition energies in this sample as determined from CER measurements. These are shown in figure 4, where the open circles correspond to the LS (feature A1 in figure 2(b)) and triangles to the VS (feature B in

figure 2(b)). The data were fitted with the popular empirical Varshini relation [18]:

$$E_g(T) = E_{g0}^V - \alpha T^2 / [\beta + T] \quad (3)$$

and also the phenomenological relation based on Bose–Einstein statistics, proposed by Vina *et al* [19]:

$$E_g(T) = E_{g0}^{BE} - 2a_{c-phn} / [\exp(E_{phn}/k_B T) - 1] \quad (4)$$

where α , β , E_{phn} , a_{c-phn} , E_{g0}^{BE} and E_{g0}^V are the fitting parameters, the last two representing the transition energy at the lowest temperature and k_B is the Boltzmann constant. The values of the fitted parameters for the LS and the VS are listed in table 1 along with those for bulk $\text{In}_{0.49}\text{Ga}_{0.51}\text{P}$ alloy.

The principal factors determining the temperature dependence of the critical point transition energies in a semiconductor are carrier–phonon interactions and thermal expansion, the former playing the dominant role [20]. In general the parameter E_{phn} is a measure of the average phonon energy and a_{c-phn} a measure of the carrier–phonon coupling strength [10]. Manoogian and Woolly [21] have shown that the parameter β in the Varshini relation can be related to the Debye temperature which is again a measure of the average phonon energy. Carrier scattering via optical phonons being dominant in III–V compounds, E_{phn} is found to be closer to but less than the LO phonon energy in bulk samples. The continuous lines in figure 4 represent fits to the data using equation (4). Approximate procedures have been adopted previously [22] to isolate the thermal expansion contribution and study the influence of carrier–phonon interactions alone. However since the thermal expansion term is not the dominant factor in the present temperature range, we did not try to subtract its contribution to the band gap change before fitting the above equations. Also the values of the fitted parameter depend somewhat on the temperature range over which the data is fitted, therefore in the present case we shall make a relative comparison of the parameters values rather than their absolute values.

A comparison of the fitted values of the parameters β and E_{phn} suggests that the average phonon energy is considerably reduced in the LS phase. The lower value of a_{c-phn} suggests that the carrier–phonon coupling strength too is reduced in the LS phase as compared to the VS phase and bulk $\text{In}_{0.49}\text{Ga}_{0.51}\text{P}$ alloy. These results, reported here for the first time, are probably additional indirect evidence for the formation of an LS due to the composition modulation. This is because as is well known in the case of superlattices, the phonon spectrum itself is modified due to the presence of confined LO phonons and folded acoustic phonons whose energies are much lower than the bulk LO phonon [23], while quantum confinement results in a weakened carrier–phonon coupling strength [24]. From the point of view of modification of the phonon spectra, the VS phase which has a periodicity of $\simeq 12 \text{ \AA}$ is closer to the $\text{In}_{0.49}\text{Ga}_{0.51}\text{P}$ alloy (periodicity $\simeq 5.65 \text{ \AA}$) than the LS phase (periodicity $\simeq 120 \text{ \AA}$) which might explain why the temperature dependence of the VS phase is similar to that of the alloy. However the above arguments need to be verified, possibly through Raman spectroscopy.

Finally we note that in figure 4 it appears that the temperature coefficients of the transition energies are not very different for the VS and the LS phases, a fact which is borne out by the relatively smaller difference in the fitted values of α for these two cases as shown in table 1. The reason for this can be seen by expanding (in the high temperature limit) the exponential term in equation (4), whereby it is easy to show that $\alpha = a_{c-phn} k_B / E_{phn}$. As both a_{c-phn} and E_{phn} are simultaneously reduced in the LS phase, their ratio (α) is not drastically affected. A reduction in the carrier–phonon interaction strength has important technological implications since it can lead to reduction in the temperature coefficient of laser emission wavelengths. However in the present case, although the carrier–phonon interaction strength seems reduced in the LS phase, the simultaneous lowering of the average phonon energy has resulted in a temperature dependence of the band gap which is not significantly smaller than that of bulk $\text{Ga}_x\text{In}_{1-x}\text{P}$ alloys.

4. Conclusion

In summary we have presented results of detailed spectroscopic study of Ga–In–P based self-organized lateral superlattices. The results have been explained by suggesting that the luminescence from these samples originates from recombination of carriers localized at excessively In rich regions within the lateral superlattice while the LCM related CER feature corresponds to transition between the minibands of the average lateral superlattice structure. These results suggest that the random alloy model needs to be improved upon and possibilities in this regard have been discussed. The temperature dependence of the transition energy of the composition modulation related CER feature seems to provide additional evidence for the presence of a lateral superlattice in these samples.

Acknowledgment

The authors would like to thank Professor K L Narsimhan for many useful discussions.

References

- [1] Millunchick J M, Twesten R D, Lee S R, Follstaedt D M, Jones E D, Ahrenkiel S P, Zhang Y, Cheong H M and Mascarenhas A 1997 *MRS Bull.* **22** 38
- [2] Hsieh K C, Baillargeon J N and Cheng K Y 1990 *Appl. Phys. Lett.* **57** 2244
- [3] Cheng K Y, Hsieh K C and Baillargeon J N 1992 *Appl. Phys. Lett.* **60** 2892
- [4] Mascarenhas A, Alonso R G, Horner G S, Froyen S, Hsieh K C and Cheng K Y 1992 *Superlatt. Microstruct.* **12** 57
- [5] Pearah P J, Chen A C, Moy A M, Hsieh K-C and Cheng K-Y 1994 *IEEE J. Quantum Electron.* **30** 608
- [6] Ghosh S, Arora B M, Kim S-J and Asahi H 1998 *Superlatt. Microstruct.* **24** 127
- [7] Kim S J, Asahi H, Takemoto M, Asami K, Takeuchi M and Gonda S-I 1996 *Japan. J. Appl. Phys.* **35** 4425
- [8] Noh J-H, Asahi H, Kim S-J, Takemoto M, Asami K and Gonda S-I 1996 *Japan. J. Appl. Phys.* **35** 3743
- [9] Ghosh S and Arora B M 1996 *Proc. Int. Conf. on Instrumentation* ed B S Ramprasad *et al* (Bangalore: New Age)

- [10] Pollak F H and Shen H 1993 *Mater. Sci. Eng. R* **10** 275
- [11] Armelles G, Munoz M C and Alonso M I 1993 *Phys. Rev. B* **47** 16 299
- [12] Bastard G 1988 *Wavemechanics Applied to Semiconductor Heterostructures* (New York: Halsted)
- [13] Marzin J Y, Charasse M N and Sermage B 1985 *Phys. Rev. B* **31** 8298
- [14] Nashiki H, Suemune I, Suzuki H and Uesugi K 1997 *Japan. J. Appl. Phys.* **36** 4199
- [15] Weber S, Limmer W, Thinke T, Sauer R, Panzlaff K, Bacher G, Meier H P and Roentgen P 1995 *Phys. Rev. B* **52** 14 739
- [16] Narukawa Y, Kawakami Y, Funato M, Fujita S, Fujita S and Nakamura S 1997 *Appl. Phys. Lett.* **70** 981
- Narukawa Y, Kawakami Y, Funato M, Fujita S, Fujita S and Nakamura S 1997 *Phys. Rev. B* **55** R1938
- [17] Tang Y, Lin H T, Rich D H, Colter P and Vernon S M 1996 *Phys. Rev. B* **53** R10 501
- Rich D H, Tang Y and Lin H T 1997 *J. Appl. Phys.* **81** 6837
- [18] Varshini Y P 1967 *Physica* **34** 149
- [19] Vina L, Logothetidis S and Cardona M 1984 *Phys. Rev. B* **30** 1979
- [20] Kim C K, Lautenschlager P and Cardona M 1986 *Solid State Commun.* **59** 797
- [21] Manoogian A and Woolly J C 1984 *Can. J. Phys.* **62** 285
- [22] Hang Z, Yan D, Pollak F H, Pettit G D and Woodall J M 1991 *Phys. Rev. B* **44** 10 546
- [23] Ivchenko E L and Pikus G 1995 *Superlattices and other Heterostructures* (Berlin: Springer)
- [24] Qiang H, Pollak F H, Sotomayor Torres C M, Leitch W, Kean A H, Stroschio M A, Lafrate G J and Kim K W 1992 *Appl. Phys. Lett.* **61** 1411